^{18}F-Flortanidazole Hypoxia PET Holds Promise as a Prognostic and Predictive Imaging Biomarker in a Lung Cancer Xenograft Model Treated with Metformin and Radiotherapy

Sven De Bruycker[1], Christel Vangestel[1,2], Tim Van den Wyngaert[1,2], Patrick Pauwels[3], Leonie wyffels[1,2], Steven Staelens[1], and Sigrid Stroobants[1,2]

[1]Molecular Imaging Center Antwerp (MICA), University of Antwerp, Wilrijk, Belgium; [2]Department of Nuclear Medicine, Antwerp University Hospital, Edegem, Belgium; and [3]Center for Oncological Research (CORE), University of Antwerp, Wilrijk, Belgium

Metformin may improve tumor oxygenation and thus radiotherapy response, but imaging biomarkers for selection of suitable patients are still under investigation. First, we assessed the effect of acute metformin administration on non–small cell lung cancer xenograft tumor hypoxia using PET imaging with the hypoxia tracer ^{18}F-flortanidazole. Second, we verified the effect of a single dose of metformin before radiotherapy on long-term treatment outcome. Third, we examined the potential of baseline ^{18}F-flortanidazole as a prognostic or predictive biomarker for treatment response. **Methods:** A549 tumor–bearing mice underwent a ^{18}F-flortanidazole PET/CT scan to determine baseline tumor hypoxia. The next day, mice received a 100 mg/kg intravenous injection of metformin. ^{18}F-flortanidazole was administered intravenously 30 min later, and a second PET/CT scan was performed to assess changes in tumor hypoxia. Two days later, the mice were divided into 3 therapy groups: controls (group 1), radiotherapy (group 2), and metformin + radiotherapy (group 3). Animals received saline (groups 1–2) or metformin (100 mg/kg; group 3) intravenously, followed by a single radiotherapy dose of 10 Gy (groups 2–3) or sham irradiation (group 1) 30 min later. Tumor growth was monitored triweekly by caliper measurement, and tumor volume relative to baseline was calculated. The tumor doubling time (TDT), that is, the time to reach twice the preirradiation tumor volume, was defined as the endpoint. **Results:** Thirty minutes after metformin treatment, ^{18}F-flortanidazole demonstrated a significant change in tumor hypoxia, with a mean intratumoral reduction in ^{18}F-flortanidazole tumor-to-background ratio (TBR) from 3.21 ± 0.13 to 2.87 ± 0.13 ($P = 0.0001$). Overall, relative tumor volume over time differed across treatment groups ($P < 0.0001$). Similarly, the median TDT was 19, 34, and 52 d in controls, the radiotherapy group, and the metformin + radiotherapy group, respectively (log-rank $P < 0.0001$). Both baseline ^{18}F-flortanidazole TBR (hazard ratio, 2.0; $P = 0.0004$) and change from baseline TBR (hazard ratio, 0.39; $P = 0.04$) were prognostic biomarkers for TDT irrespective of treatment, and baseline TBR predicted metformin-specific treatment effects that were dependent on baseline tumor hypoxia. **Conclusion:** Using ^{18}F-flortanidazole PET imaging in a non–small cell lung cancer xenograft model, we showed that metformin may act as a radiosensitizer by increasing tumor oxygenation and that baseline ^{18}F-flortanidazole shows promise as an imaging biomarker.

Key Words: ^{18}F-HX4 PET; tumor hypoxia; metformin; radiotherapy; imaging biomarkers

J Nucl Med 2019; 60:34–40
DOI: 10.2967/jnumed.118.212225

Tumor hypoxia is a negative prognostic factor for radiation-treated tumors, including non–small cell lung cancer (NSCLC) (*1*). Hypoxia is often described as chronic (i.e., the result of diffusion limitations) or acute (i.e., the result of transient fluctuations in blood flow), although more granular classifications have been proposed (*2*). Hypoxia causes radiotherapy resistance primarily by limiting oxygen fixation, the crucial step for radiation to effect DNA damage and, importantly, has also been linked with a more aggressive tumor phenotype as such (*3*). Yet, most interventions to ameliorate tumor oxygenation have failed translation into routine clinical practice (*4*), except for nimorazole, an oxygen-mimicking radiosensitizer that has been incorporated into standard radiotherapy for head and neck cancer in Denmark only (*3*).

More recent studies have focused on the radiosensitizing properties of metformin, a first-line treatment for diabetes mellitus, because retrospective analyses have found that diabetic patients with cancer who underwent radiotherapy had better outcomes if they were taking metformin than not (*5–7*). These intriguing observations were later confirmed in nondiabetic preclinical models (*8,9*). Metformin may affect tumor therapy response and tumor growth either directly or indirectly. The direct effect is attributed to the inhibition of the mitochondrial complex I and its downstream pathways, resulting in activation of the cellular energy sensor adenosine monophosphate–activated kinase. This activation in turn increases cellular catabolism and reduces anabolism (*10*). The indirect effect, on the other hand, is caused by metformin's lowering effects on blood glucose and insulin levels, two major factors stimulating cancer growth. Yet, the way in which metformin influences radiation response is still controversial and may probably be a result of different mechanisms (*5–7*). One of the better-established theories is that metformin can acutely reduce tumor hypoxia by inhibiting the mitochondrial respiratory chain,

Received Mar. 30, 2018; revision accepted Jun. 23, 2018.
For correspondence or reprints contact: Sigrid Stroobants, Department of Nuclear Medicine, Antwerp University Hospital, Wilrijkstraat 10, 2650 Edegem, Belgium.
E-mail: sigrid.stroobants@uza.be
Published online Jul. 6, 2018.

lowering cellular oxygen consumption and thus reoxygenating hypoxic cells (*9*). In line with this theory, metformin has been shown to inhibit the hypoxia-driven activation of transcription factor hypoxia-inducible factor-1, which is normally upregulated under hypoxic conditions and decreases the susceptibility of cancer cells to apoptosis by promoting progression and proliferation (*11*).

The validation of appropriate radiotracers as imaging biomarkers for patient selection, critically needed for further progress with clinical trials using metformin as a radiosensitizer, is still ongoing (*12*). The most widely spread hypoxia PET tracers are the ^{18}F-labeled 2-nitroimidazoles. Only under hypoxic conditions do those molecules undergo a series of intracellular reductions that result in intermediate metabolites with the ability to bind intracellular macromolecules. Despite the fact that 2-nitroimidazole–based tracers may detect mainly chronic rather than acute hypoxia, it has been shown in different clinical trials that tumors with a higher tracer uptake generally show a poorer radiotherapy response (*13*). Currently, ^{18}F-flortanidazole is an established tool in this setting with correlations between tumoral uptake and reference standard immunohistochemistry markers of hypoxia (*14–16*), and with a more favorable kinetic profile than earlier 2-nitroimidazole–based hypoxia PET tracers (*15*). Despite its successful translation into human use in various cancer types, including NSCLC, questions remain on how ^{18}F-flortanidazole can be incorporated in treatment decision making of hypoxia-modulating therapies (*17*). Therefore, we investigated the effect of acute metformin administration on NSCLC xenograft tumor hypoxia using ^{18}F-flortanidazole, studied the effect of a single dose of metformin before radiotherapy on outcome, and examined the potential of baseline ^{18}F-flortanidazole PET as a biomarker of overall and metformin-specific treatment response.

MATERIALS AND METHODS

Animal Model

The experimental protocol was approved by the Antwerp University Ethical Committee for Animal Experiments (2015-42), and all applicable institutional and European guidelines for the care and use of animals were followed. Female CD-1 athymic nude mice (n = 36; Charles Rivers Laboratories) were group-housed (up to 6 animals per cage) in individually ventilated cages under a 12-h:12-h dark:light cycle, controlled temperature (20°C–23°C), and controlled humidity (50%–60%) with ad libitum access to standard laboratory chow and water.

A549 NSCLC cells (ATCC) were cultured as monolayers in Dulbecco modified Eagle medium enriched with 10% fetal bovine serum, 2 mM L-glutamine, 1 mM sodium pyruvate, and 1% penicillin-streptomycin (Invitrogen) at 37°C and 5% CO_2 in a humidified incubator. Cultures were maintained in exponential growth. A549 cells were harvested by trypsinization with 0.05% trypsin-ethylenediaminetetraacetic acid, washed 2 times with sterile phosphate-buffered saline, counted using the Muse Cell Count and Viability Assay (Merck Millipore), and resuspended in sterile phosphate-buffered saline at a concentration of 5×10^7 viable cells per milliliter. Mice (n = 30) at an age of 7–9 wk were inoculated with 100 μL of A549 cell suspension in both hind legs. Tumor growth was evaluated 3 times per week with digital caliper measurements from the moment the tumors became palpable. Tumor volume was calculated with the formula $0.5 \times (\text{length} \times \text{width}^2)$. Relative tumor volumes (RTVs) with respect to baseline were calculated. The tumor doubling time (TDT), that is, the time to reach twice the preirradiation tumor volume, was used as a proxy for progression-free survival and was defined as the endpoint. A minimum tumor volume of 100 mm^3 was required at the start of the study. Two animals reached ethical endpoints not related to the TDT before the end of the study and were therefore euthanized and also excluded from further analysis.

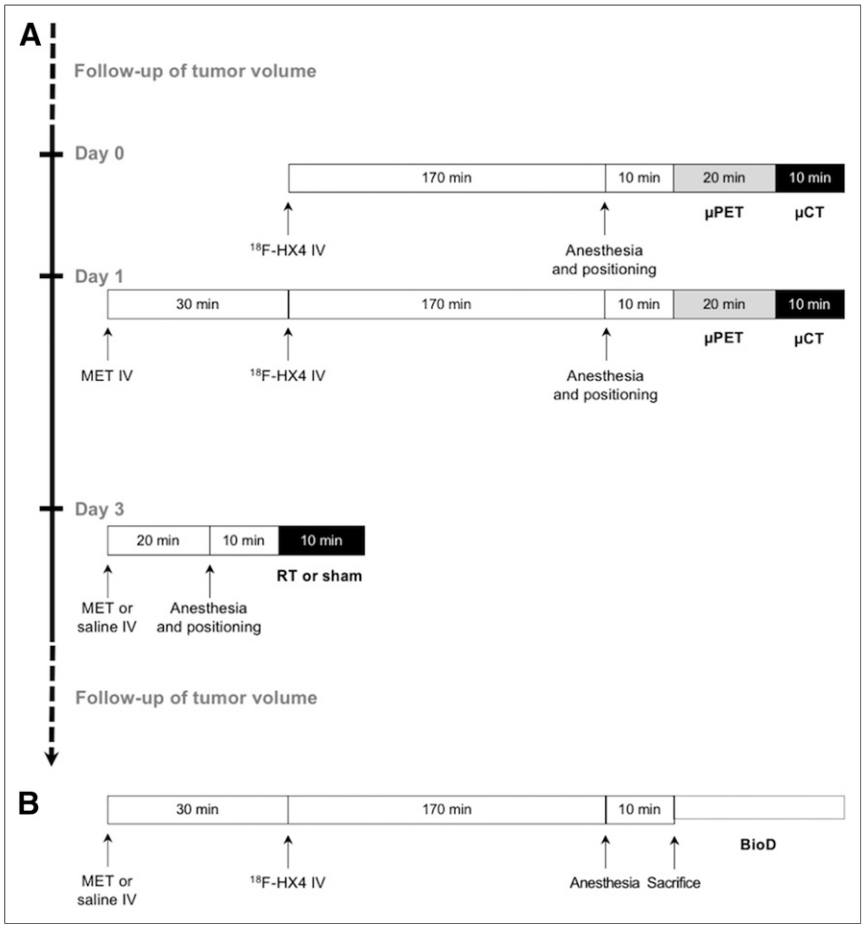

FIGURE 1. Experimental setup. (A) Acute metformin administration in A549 xenografts. (B) Biodistribution study. Hypoxia was quantified using ^{18}F-flortanidazole. BioD = biodistribution study; ^{18}F-HX4 = ^{18}F-flortanidazole; IV = intravenous; μ = small-animal; MET = metformin; RT = radiotherapy.

Tracer Production

^{18}F-flortanidazole was prepared in an automated synthesis module (Fluorsynthon I; Comecer) by reaction of azeotropically dried ^{18}F-K(K_{222})F with 17–20 mg of flortanidazole precursor (Syncom) dissolved in a 50:50 mixture of t-butanol:acetonitrile at 110°C for 6 min. After the fluorination, acetonitrile was removed under a stream of helium and a vacuum, and 0.1 M HCl (1 mL)

was added for acidic hydrolysis at 90°C for 5 min. After the reaction had been cooled to 75°C, 0.7 mL of 2 M NaOAc, pH 5.5, was added, and the mixture was loaded onto a high-pressure liquid chromatography loop through a preconditioned Alumina N Light cartridge (Waters). ^{18}F-flortanidazole was purified using a Luna C18(2) 250 × 10 mm, 10-μm high-pressure liquid chromatography column (Phenomenex) and 9% ethanol in saline as the mobile phase at a flow rate of 3 mL/min. The fraction containing ^{18}F-flortanidazole was collected and transferred to a shielded laminar flow cabinet, where it was diluted with saline containing 2% ascorbic acid and sterile-filtered (25-mm syringe filter, 0.2-μm polyethersulfone membrane; VWR International).

^{18}F-flortanidazole was obtained with a radiochemical purity of more than 95% and a radiochemical yield of 47% ± 5% (decay-corrected to end of bombardment; n = 7). The molar activity was 137.3 ± 12.6 GBq/μmol (decay-corrected to end of synthesis; n = 7).

Experimental Setup

Acute Metformin Administration and Its Radiosensitizing Effects. The study design is shown in Figure 1. A baseline ^{18}F-flortanidazole PET/CT scan was performed to determine baseline tumor hypoxia (day 0). Details of the scan protocol are represented in Figure 1A. Approximately 18.5 MBq of ^{18}F-flortanidazole in a final volume of 200 μL of saline were administered as a bolus injection via the tail vein. During the acquisition, which started 180 min after tracer administration (*18*), the mice were anesthetized with isoflurane (induction, 5%; maintenance, 1%–2%; Abbott) and medical O_2 (100%), body temperature was kept constant via a heating bed, and respiration was continuously monitored. A static PET acquisition (20 min) followed by an anatomic CT acquisition (10 min) was performed on an Inveon small-animal PET/CT scanner (Siemens Preclinical Solutions). The next day, the mice were given a 100 mg/kg dose of metformin hydrochloride (ABC Chemicals) in a final volume of 100 μL of saline intravenously. Thirty minutes later, the mice were injected with approximately 18.5 MBq of ^{18}F-flortanidazole intravenously, whereupon a second ^{18}F-flortanidazole PET/CT scan was performed to assess changes in tumor hypoxia.

PET images were reconstructed using 4 iterations × 16 subsets of a 3-dimensional ordered-subset expectation-maximization algorithm after Fourier rebinning. Normalization, as well as correction for dead time, scatter, and attenuation, was applied. The PET/CT images were analyzed in PMOD software (version 3.3; PMOD Technologies). An elliptic volume of interest that enclosed the entire tumor was positioned manually and was centered on the tumor area that showed maximal uptake. Then, 3-dimensional isocontours at 60% of the maximum pixel value within this elliptic volume of interest were generated automatically. Tumor-to-background ratios (TBRs) were determined using the heart as the reference region, with the heart being manually delineated on the CT images of each mouse.

Two days later, the mice were categorized into a control group (group 1; n = 7), a radiotherapy group (group 2; n = 6), and a metformin + radiotherapy group (group 3; n = 8). The animals were administered saline (groups 1–2) or a 100 mg/kg dose of metformin hydrochloride (group 3) intravenously, and a single dose of radiotherapy was administered to groups 2 and 3 at 30 min after metformin treatment. The control animals received sham irradiation. In brief, during irradiation the animals were anesthetized with isoflurane (5% for induction, 1%–2% for maintenance) and positioned within the self-contained x-ray system X-RAD 320 (Precision X-Ray). The whole body of the animals was shielded using lead, except for the tumors. Irradiation was delivered at a rate of 100 cGy/min with 320-kV x-rays. Tumors received a single dose of 10 Gy. Control animals that received sham irradiation were anesthetized and positioned in the x-ray system for 10 min but were not irradiated. After irradiation, growth of tumors was monitored until they reached a volume of 1,500 mm^3 (the ethical endpoint of the study), whereupon the animals were euthanized and tumor tissue was resected, formalin-fixed, and paraffin-embedded. Tissue sections 3 μm thick were mounted on SuperFrost microscope slides (Menzel-Glaser) for hematoxylin and eosin staining and Ki-67 immunohistochemistry. Immunostaining and scoring were performed as previously described (*19*).

^{18}F-Flortanidazole Biodistribution Analysis. To rule out the possibility that metformin altered ^{18}F-flortanidazole uptake by disturbing its biodistribution, a ^{18}F-flortanidazole ex vivo study was performed on 6 mice (Fig. 1B). In brief, nude mice were injected intravenously with either a 100 mg/kg dose of metformin (n = 3) or saline (n = 3), followed 30 min later by approximately 18.5 MBq of ^{18}F-flortanidazole. After a 170-min delay, the mice were anesthetized with isoflurane, and 10 min later blood was collected by cardiac puncture, immediately followed by killing of the animals by cervical dislocation. All main organs and tissues were rapidly removed, rinsed in phosphate-buffered saline, blotted dry, weighed, and counted for radioactivity in an automated Wizard^2 2480 γ-counter (PerkinElmer). Activity was expressed as percentage injected dose per gram of sample (%ID/g).

Statistics

Prism software (version 6; GraphPad Software) was applied to analyze changes in ^{18}F-flortanidazole uptake using a Wilcoxon matched-pairs signed-rank test and to analyze differences in parameters between groups using log-rank tests or a Kruskal–Wallis test with Mann–Whitney U post hoc analyses. Using SAS System software (version 9; SAS Institute Inc.), a general linear mixed model including time, treatment group, and their interaction with step-down Bonferroni adjustment for post hoc multiple comparison was performed to determine whether the treatment had a significant effect on the RTVs. Cox proportional-hazards regression was applied to assess the effect of treatment and ^{18}F-flortanidazole uptake on TDT (Stata 14.2; StataCorp LLC). Metformin-specific effects

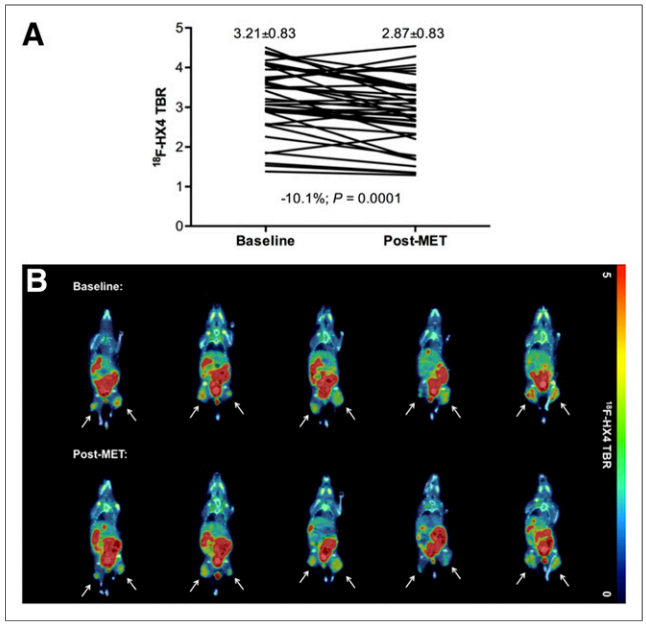

FIGURE 2. Metformin improves tumor oxygenation. (A) Significant decrease in ^{18}F-flortanidazole TBR could be observed 30 min after intravenous administration of metformin (100 mg/kg; P = 0.0001). (B) Representative ^{18}F-flortanidazole PET/CT TBR-corrected images (coronal view) of 5 mice before (upper row) and after (lower row) metformin administration. Arrows indicate tumors. ^{18}F-HX4 = ^{18}F-flortanidazole; MET = metformin.

TABLE 1
Overview of Baseline Parameters of Different Treatment Groups of A549 Xenografts

Parameter	Radiotherapy	Metformin + radiotherapy	Control	*P*
Tumor volume (mm^3)	395 ± 57	297 ± 51	329 ± 65	0.5
Animal weight (g)	29.6 ± 0.8	29.7 ± 0.9	29.4 ± 1.1	1.0
Baseline ^{18}F-flortanidazole TBR	3.60 ± 0.17	2.74 ± 0.26	3.47 ± 0.20	0.3
Δ^{18}F-flortanidazole TBR (%)	−13 ± 4	−4 ± 4	−14 ± 3	0.2

Δ^{18}F-flortanidazole TBR = change in ^{18}F-flortanidazole TBR after metformin.
Data are expressed as mean ± SEM.

were assessed by estimating the interaction term of treatment and ^{18}F-flortanidazole uptake. Model checks for goodness of fit and proportional-hazards assumption were performed as appropriate. *P* values of less than 0.05 were considered statistically significant. All data are expressed as mean ± SEM.

RESULTS

Acute Metformin Administration and Its Radiosensitizing Effects

The mean tumor volume at baseline was 342 ± 33 mm^3. Thirty minutes after metformin treatment, ^{18}F-flortanidazole TBR could demonstrate a significant change in A549 tumor hypoxia, with a mean intratumoral reduction in ^{18}F-flortanidazole TBR from 3.21 ± 0.83 to 2.87 ± 0.83 ($P = 0.0001$), as depicted in Figure 2A. Importantly, the background tracer uptake was not affected by metformin (0.06 ± 0.01 to 0.07 ± 0.01; $P = 0.09$). Representative baseline and follow-up ^{18}F-flortanidazole images of 5 mice are shown in Figure 2B.

Two days after their follow-up scan, the animals were divided into 3 treatment groups with comparable baseline parameters, summarized in Table 1. The tumor growth curves of the A549 xenografts are shown in Figure 3A. Overall, RTVs over time differed across treatment groups ($P < 0.0001$), with the metformin + radiotherapy group having significantly lower RTVs than controls from day 7 after therapy onward (0.68 ± 0.05 vs. 1.43 ± 0.08, respectively; $P = 0.006$) and the metformin + radiation-treated tumors having significantly lower RTVs than radiation-treated tumors from day 12 after therapy onward (0.77 ± 0.06 vs. 1.27 ± 0.08, respectively; $P = 0.03$). From that time, the RTVs of radiation-treated tumors were also significantly lower than control tumor RTVs (1.65 ± 0.13; $P = 0.01$). These results were confirmed by log-rank tests, which found a significant increase in the median doubling-free survival of radiation-treated animals compared with controls (34 vs. 19 d, respectively; 95% confidence interval [CI], 3.0–18.8; log-rank $P = 0.0002$). Addition of metformin to the treatment regimen, compared with radiotherapy alone, further increased the median doubling-free survival to 52 d (95% CI, 1.7–11.3; log-rank $P = 0.005$), as clearly shown in Figure 3B. At the time the animals were killed, tumor proliferation as assessed with Ki-67 immunohistochemistry was numerically higher in controls (55% ± 2%) than in radiation-treated tumors (51% ± 2%) or in metformin + radiation-treated tumors (47% ± 3%; $P = 0.2$; Fig. 4A). Accordingly, necrosis was numerically lower in control tumors (34% ± 7%) than in radiation-treated tumors (42% ± 9%) or in metformin + radiation-treated tumors (42% ± 7%; $P = 0.6$; Fig. 4B). No correlations were found between the immunohistochemistry parameters and the volumetric outcome parameters (i.e., RTV and TDT; data not shown). Figures 4C and 4D show representative immunohistochemistry images.

^{18}F-Flortanidazole as a Biomarker of TDT

Overall, baseline ^{18}F-flortanidazole TBR was a prognostic biomarker for TDT, independent of treatment and adjusting for baseline

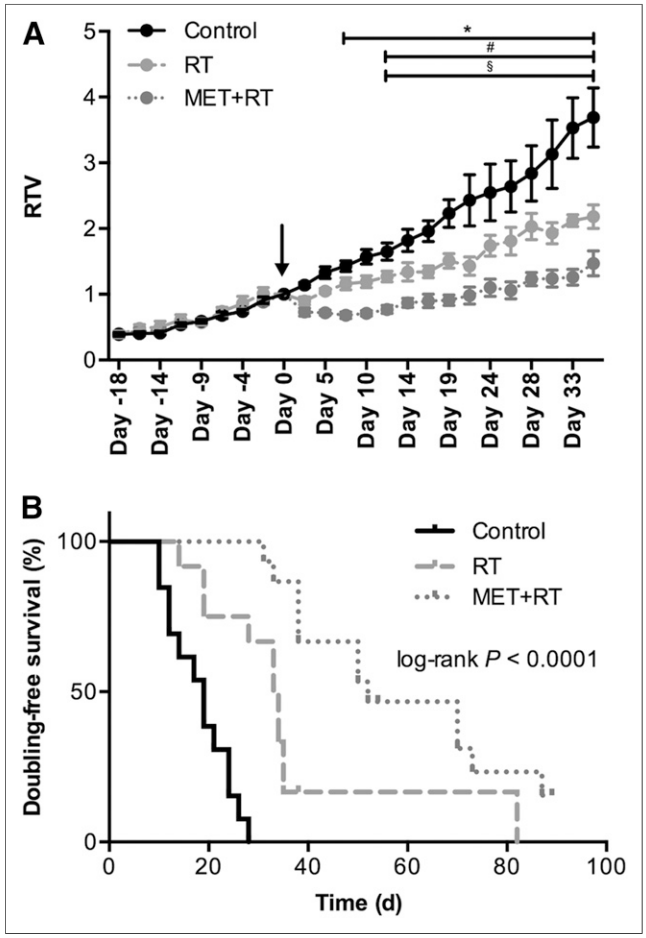

FIGURE 3. Metformin improves radiotherapy response in A549 tumors. (A) Tumor growth was followed, and RTVs were calculated. Arrow indicates moment of therapy administration. (B) Kaplan–Meier representation of doubling-free survival time (overall log-rank $P < 0.0001$). *Significant difference between metformin + radiotherapy and control. #Significant difference between metformin + radiotherapy and radiotherapy. §Significant difference between radiotherapy and control. MET = metformin; RT = radiotherapy.

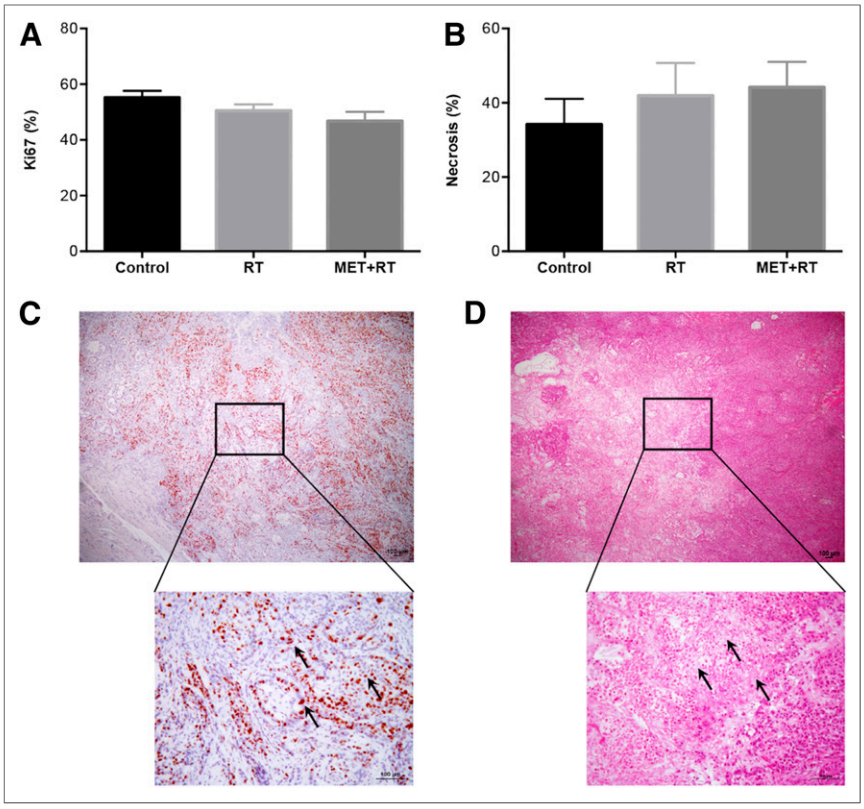

FIGURE 4. Tumor proliferation as assessed with Ki-67 immunohistochemistry and tumor necrosis at sacrifice. (A) No major differences in tumor proliferation could be observed between different treatment groups. (B) Same conclusions could be drawn from necrosis scoring. (C) Representative example of Ki-67 staining. Arrows indicate positively stained nuclei. (D) Representative example of hematoxylin and eosin staining. Arrows indicate areas of necrosis. MET = metformin; RT = radiotherapy.

tumor volume (hazard ratio, 2.0 for every unit increase in TBR; 95% CI, 1.2–3.2; $P = 0.0004$). In addition, a reduction in TBR of at least 5% (Δ^{18}F-flortanidazole) after metformin administration was also prognostic for TDT across treatment groups (hazard ratio, 0.39; 95% CI, 0.16–0.95; $P = 0.04$). Of these two, baseline ^{18}F-flortanidazole performed slightly better than Δ^{18}F-flortanidazole TBR in predicting TDT (0.86 on the Harrell concordance index and a 95% CI of 0.81–0.91, vs. 0.81 and 0.76–0.85, respectively; $P = 0.02$).

As clearly shown in Figure 5, which focuses specifically on the treatment effect of metformin, baseline ^{18}F-flortanidazole TBR could predict the synergistic effect of metformin + radiotherapy over radiotherapy alone, revealing that treatment modulation was dependent on baseline tumor hypoxia. Across the spectrum of observed baseline hypoxia values, adding metformin to radiotherapy for tumors with lower ^{18}F-flortanidazole TBRs (≤2.5) resulted in a relative reduction of 72% in the risk of tumor doubling over radiotherapy alone (hazard ratio, 0.28; 95% CI, 0.09–0.92; $P = 0.04$), whereas this modulatory effect was attenuated in tumors at the higher end of baseline TBRs (>2.5) (hazard ratio, 0.55; 95% CI, 0.11–2.82; $P = 0.5$).

^{18}F-Flortanidazole Biodistribution Analysis

In both the metformin-treated group and the control group, the quantitative ^{18}F-flortanidazole biodistribution study 180 min after injection showed a high accumulation of radioactivity in urine (0.23 ± 0.14 vs. 0.92 ± 0.31 %ID, respectively) and the large intestine (2.36 ± 0.26 vs. 2.66 ± 0.24 %ID/g, respectively), indicating a combined renal and intestinal clearance. Blood-pool activity was very low (0.05 ± 0.00 vs. 0.07 ± 0.02 %ID/g, respectively). Figure 6 shows that in general, no significant differences in the ^{18}F-flortanidazole biodistribution profile could be observed between the metformin-treated mice and the control group.

DISCUSSION

In an A549 NSCLC xenograft model, we first looked at changes in intratumoral hypoxia after acute metformin administration and found a mean reduction in ^{18}F-flortanidazole uptake of more than 10%, implying that a single dose of metformin can immediately improve tumor oxygenation. Our result is in line with previous observations in a colorectal cancer xenograft model, in which uptake of the hypoxia tracer ^{18}F-fluoroazomycin arabinoside was compared between tumors given intravenous metformin and tumors given intravenous saline (*9*).

Second, we observed that administration of metformin 30 min before radiotherapy significantly improved long-term treatment outcome. Others made similar observations in the colorectal cancer xenograft model (*9*). In an A549 xenograft model, a study had already found that long-term daily administration of metformin, 300 mg/kg, via the drinking water sensitized tumors to the effects of a single radiotherapy dose of 10 Gy (*8*), but to date the effects of a single dose of metformin on radiotherapy outcome has not been explored in A549 tumors.

It has been hypothesized that metformin can accumulate up to 500-fold in the mitochondria, resulting in mitochondrial concentrations in the millimolar range (*20,21*), which should be adequate for inhibiting the respiratory chain complex I (*11,20,22*) and consequently improving tumor oxygenation.

Despite our own definite observations in line with this theory, the direct inhibition of tumor cell respiration by biguanides has lately been questioned. A recent study showed that tumor retention of an intraperitoneally administered mixture of unlabeled metformin and trace amounts of ^{11}C-labeled metformin (^{11}C-metformin; total dose equaling 250 mg/kg) was low and did not affect tumor hypoxia. Moreover, the same study showed that an intravenously administered bolus of ^{11}C-metformin cleared rapidly from the circulation (*23*). These authors extrapolated their observations to a metformin dose of 100 mg/kg (which we used in our setup) and concluded that the resulting 50 μM plasma levels 30 min after administration are insufficient to evoke direct respiratory responses (*23*). However, they compared in vitro and in vivo observations, and we believe such a comparison can be misleading because ample evidence shows the existence of different dynamics of response to metformin in cell cultures and in vivo (*21*).

We demonstrated that a higher tumoral baseline ^{18}F-flortanidazole uptake significantly correlated with a poorer survival independently

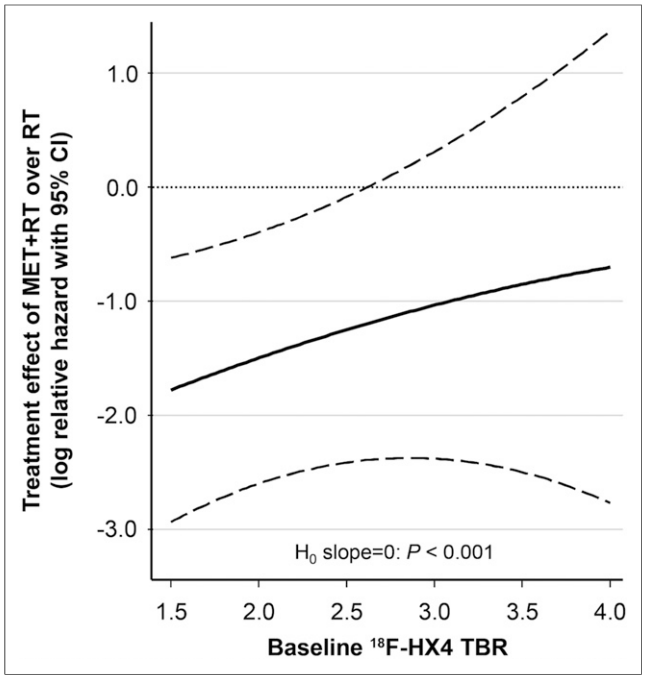

FIGURE 5. Therapeutic benefit of metformin was dependent on baseline degree of tumor hypoxia and could be predicted with baseline ^{18}F-flortanidazole PET. ^{18}F-HX4 = ^{18}F-flortanidazole; H_0 = null hypothesis; MET = metformin; RT = radiotherapy.

from the therapy that was administered, supporting ^{18}F-flortanidazole as a prognostic biomarker in the A549 xenograft model. This observation confirms previous clinical findings for other 2-nitroimidazole PET imaging in different types of cancer, including NSCLC (*1,13,24*). However, to the best of our knowledge, the potential of the pharmacokinetically superior hypoxia PET tracer ^{18}F-flortanidazole as a prognostic biomarker has not been assessed to date (*25,26*).

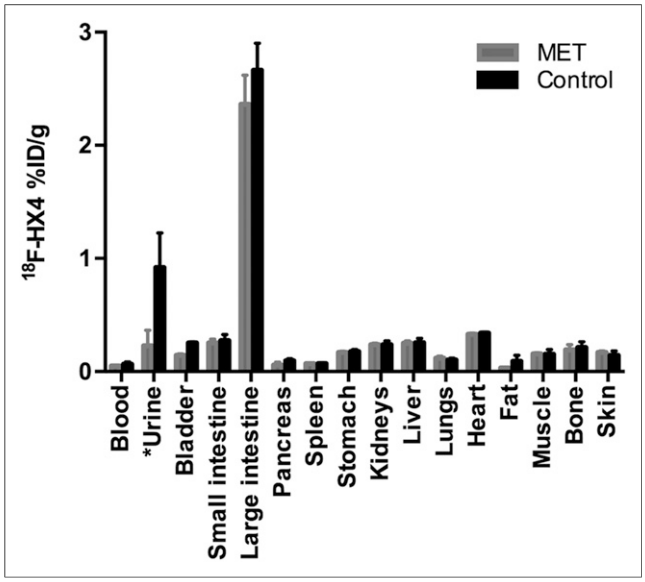

FIGURE 6. Results of ^{18}F-flortanidazole biodistribution study after acute metformin administration. No major differences could be observed in ^{18}F-flortanidazole biodistribution profile between metformin-treated mice and control group. ^{18}F-HX4 = ^{18}F-flortanidazole; MET = metformin. *Values are shown as %ID because of variability in urine production.

Interestingly, we also found ^{18}F-flortanidazole PET to be a predictive biomarker for metformin-specific therapeutic effects. In other words, the therapeutic benefit of metformin + radiotherapy over radiotherapy alone in our setup was found to be dependent on the baseline degree of tumor hypoxia and to be most pronounced in tumors with lower values of baseline ^{18}F-flortanidazole TBR ($\leq$2.5). There are some potential explanations for this apparent differential therapeutic effect of metformin. First, the administered dose or the applied therapy regimen may have been inadequate, particularly for tumors with a higher degree of baseline hypoxia in which the increase in tumor oxygenation resulting from metformin may still be too limited for effective radiosensitizing effects. Second, it is well established that mitochondrial inhibition by metformin not only results in more oxygen in cancer cells but also activates the adenosine monophosphate–activated kinase pathway, which eventually results in inhibition of mammalian target of rapamycin, a central regulator of cell growth and survival. In this way, metformin may suppress tumor proliferation independently from hypoxia (*5,7*). However, under highly hypoxic conditions, metformin may be unable to activate adenosine monophosphate–activated kinase or to inhibit mammalian target of rapamycin (*27*). Taken together, ^{18}F-flortanidazole shows great promise as a tool to investigate and predict metformin-specific therapeutic effects and tailor patient treatment selection.

However, on top of the complex drug dynamics and kinetics that are not fully understood yet, our study design may have been limited by the high baseline degree of tumor hypoxia. The baseline ^{18}F-flortanidazole TBR was at least 1.4 for all tumors, and TBR thresholds of as low as 1.2 have been reported to represent hypoxia, limiting our ability to fully assess treatment-specific effects across the entire range of tumor oxygenation (*28–30*). Indeed, Graves et al. have shown that ^{18}F-fluoroazomycin arabinoside uptake could be detected in only subcutaneous, not orthotopic, A549 NSCLC xenograft models (*31*). The accessibility of oxygen via the alveoli in orthotopic, but not subcutaneous, lung tumors may explain this phenomenon (*32*).

CONCLUSION

Using ^{18}F-flortanidazole PET in an NSCLC xenograft model, we demonstrated that tumor hypoxia significantly decreased immediately after intravenous administration of a single dose of metformin. Administering metformin before irradiation significantly increased TDT. Additionally, we demonstrated that baseline ^{18}F-flortanidazole PET shows great promise as an imaging biomarker—being both prognostic for survival and predictive for metformin-specific therapeutic effects.

DISCLOSURE

No potential conflict of interest relevant to this article was reported.

ACKNOWLEDGMENTS

We thank Caroline Berghmans, Philippe Joye, and Christophe Hermans for providing technical assistance; Dominique Vanderghinste and István Kerstész for producing the ^{18}F-flortanidazole; and Joseph Walsh for engaging in useful discussions on the radiochemistry.

REFERENCES

1. Grootjans W, de Geus-Oei L-F, Troost EGC, Visser EP, Oyen WJG, Bussink J. PET in the management of locally advanced and metastatic NSCLC. *Nat Rev Clin Oncol.* 2015;12:395–407.
2. Bayer C, Shi K, Astner ST, Maftei C-A, Vaupel P. Acute versus chronic hypoxia: why a simplified classification is simply not enough. *Int J Radiat Oncol Biol Phys.* 2011;80:965–968.
3. Siemann DW, Horsman MR. Modulation of the tumor vasculature and oxygenation to improve therapy. *Pharmacol Ther.* 2015;153:107–124.
4. Overgaard J. Hypoxic radiosensitization: adored and ignored. *J Clin Oncol.* 2007;25:4066–4074.
5. Koritzinsky M. Metformin: a novel biological modifier of tumor response to radiation therapy. *Int J Radiat Oncol Biol Phys.* 2015;93:454–464.
6. Samsuri NAB, Leech M, Marignol L. Metformin and improved treatment outcomes in radiation therapy: a review. *Cancer Treat Rev.* 2017;55:150–162.
7. Lin A, Maity A. Molecular pathways: a novel approach to targeting hypoxia and improving radiotherapy efficacy via reduction in oxygen demand. *Clin Cancer Res.* 2015;21:1995–2000.
8. Storozhuk Y, Hopmans SN, Sanli T, et al. Metformin inhibits growth and enhances radiation response of non-small cell lung cancer (NSCLC) through ATM and AMPK. *Br J Cancer.* 2013;108:2021–2032.
9. Zannella VE, Dal Pra A, Muaddi H, et al. Reprogramming metabolism with metformin improves tumor oxygenation and radiotherapy response. *Clin Cancer Res.* 2013;19:6741–6750.
10. Makowski L, Hayes DN. Role of LKB1 in lung cancer development. *Br J Cancer.* 2008;99:683–688.
11. Wheaton WW, Weinberg SE, Hamanaka RB, et al. Metformin inhibits mitochondrial complex I of cancer cells to reduce tumorigenesis. *eLife.* 2014;3:e02242.
12. Troncone M, Cargnelli SM, Villani LA, et al. Targeting metabolism and AMP-activated kinase with metformin to sensitize non-small cell lung cancer (NSCLC) to cytotoxic therapy: translational biology and rationale for current clinical trials. *Oncotarget.* 2017;8:57733–57754.
13. Horsman MR, Mortensen LS, Petersen JB, Busk M, Overgaard J. Imaging hypoxia to improve radiotherapy outcome. *Nat Rev Clin Oncol.* 2012;9:674–687.
14. Dubois LJ, Lieuwes NG, Janssen MHM, et al. Preclinical evaluation and validation of [^{18}F]HX4, a promising hypoxia marker for PET imaging. *Proc Natl Acad Sci USA.* 2011;108:14620–14625.
15. Carlin S, Zhang H, Reese M, Ramos NN, Chen Q, Ricketts SA. A comparison of the imaging characteristics and microregional distribution of 4 hypoxia PET tracers. *J Nucl Med.* 2014;55:515–521.
16. Wack LJ, Mönnich D, van Elmpt W, et al. Comparison of [^{18}F]-FMISO, [^{18}F]-FAZA and [^{18}F]-HX4 for PET imaging of hypoxia: a simulation study. *Acta Oncol.* 2015;54:1370–1377.
17. Challapalli A, Carroll L, Aboagye EO. Molecular mechanisms of hypoxia in cancer. *Clin Transl Imaging.* 2017;5:225–253.
18. Peeters SGJA, Zegers CML, Lieuwes NG, et al. A comparative study of the hypoxia PET tracers [^{18}F]HX4, [^{18}F]FAZA, and [^{18}F]FMISO in a preclinical tumor model. *Int J Radiat Oncol Biol Phys.* 2015;91:351–359.
19. De Bruycker S, Vangestel C, Van den Wyngaert T, et al. Baseline [^{18}F]FMISO μPET as a predictive biomarker for response to HIF-1α inhibition combined with 5-FU chemotherapy in a human colorectal cancer xenograft model. *Mol Imaging Biol.* 2016;18:606–616.
20. Chandel NS, Avizonis D, Reczek CR, et al. Are metformin doses used in murine cancer models clinically relevant? *Cell Metab.* 2016;23:569–570.
21. Dowling RJO, Lam S, Bassi C, et al. Metformin pharmacokinetics in mouse tumors: implications for human therapy. *Cell Metab.* 2016;23:567–568.
22. He L, Wondisford FE. Metformin action: concentrations matter. *Cell Metab.* 2015;21:159–162.
23. Iversen AB, Horsman MR, Jakobsen S, et al. Results from ^{11}C-metformin-PET scans, tissue analysis and cellular drug-sensitivity assays questions the view that biguanides affects tumor respiration directly. *Sci Rep.* 2017;7:9436.
24. Bollineni VR, Wiegman EM, Pruim J, Groen HJM, Langendijk JA. Hypoxia imaging using positron emission tomography in non-small cell lung cancer: implications for radiotherapy. *Cancer Treat Rev.* 2012;38:1027–1032.
25. Yip C, Blower PJ, Goh V, Landau DB, Cook GJR. Molecular imaging of hypoxia in non-small-cell lung cancer. *Eur J Nucl Med Mol Imaging.* 2015;42:956–976.
26. Szyszko TA, Yip C, Szlosarek P, Goh V, Cook GJR. The role of new PET tracers for lung cancer. *Lung Cancer.* 2016;94:7–14.
27. Garofalo C, Capristo M, Manara MC, et al. Metformin as an adjuvant drug against pediatric sarcomas: hypoxia limits therapeutic effects of the drug. *PLoS One.* 2013;8:e83832.
28. Busk M, Horsman MR, Overgaard J. Resolution in PET hypoxia imaging: voxel size matters. *Acta Oncol.* 2008;47:1201–1210.
29. Michalski MH, Chen X. Molecular imaging in cancer treatment. *Eur J Nucl Med Mol Imaging.* 2011;38:358–377.
30. Even AJG, Reymen B, La Fontaine MD, et al. Predicting tumor hypoxia in non-small cell lung cancer by combining CT, FDG PET and dynamic contrast-enhanced CT. *Acta Oncol.* 2017;56:1591–1596.
31. Graves EE, Vilalta M, Cecic IK, et al. Hypoxia in models of lung cancer: implications for targeted therapeutics. *Clin Cancer Res.* 2010;16:4843–4852.
32. Maity A, Koumenis C. Location, location, location: makes all the difference for hypoxia in lung tumors. *Clin Cancer Res.* 2010;16:4685–4687.